

# Chapter 1

## Contact Mechanics

### 1.1 Introduction

There has been considerable recent interest in the mechanical characterisation of thin film systems and small volumes of material using depth-sensing indentation tests with either spherical or pyramidal indenters. Usually, the principal goal of such testing is to extract elastic modulus and hardness of the specimen material from experimental readings of indenter load and depth of penetration. These readings give an indirect measure of the area of contact at full load, from which the mean contact pressure, and thus hardness, may be estimated. The test procedure, for both spheres and pyramidal indenters, usually involves an elastic-plastic loading sequence followed by an unloading. The validity of the results for hardness and modulus depends largely upon the analysis procedure used to process the raw data. Such procedures are concerned not only with the extraction of modulus and hardness, but also with correcting the raw data for various systematic errors that have been identified for this type of testing. The forces involved are usually in the millinewton ( $10^{-3}$  N) range and are measured with a resolution of a few nanonewtons ( $10^{-9}$  N). The depths of penetration are on the order of microns with a resolution of less than a nanometre ( $10^{-9}$  m). In this chapter, the general principles of elastic and elastic-plastic contact and how these relate to indentations at the nanometre scale are considered.

### 1.2 Elastic Contact

The stresses and deflections arising from the contact between two elastic solids are of particular interest to those undertaking indentation testing. The most well-known scenario is the contact between a rigid sphere and a flat surface as shown in Fig. 1.1.

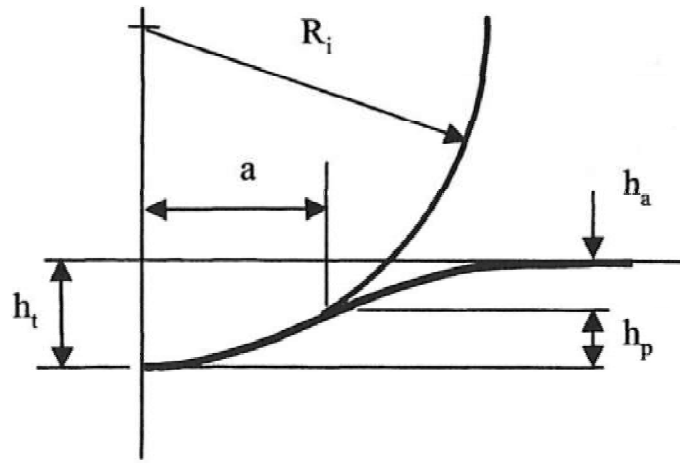


**Fig. 1.1** Schematic of contact between a rigid indenter and a flat specimen with modulus  $E$ . The radius of the circle of contact is  $a$ , and the total depth of penetration is  $h_t$ .  $h_a$  is the depth of the circle of contact from the specimen free surface, and  $h_p$  is the distance from the bottom of the contact to the contact circle.

Hertz<sup>1,2</sup> found that the radius of the circle of contact  $a$  is related to the indenter load  $P$ , the indenter radius  $R$ , and the elastic properties of the contacting materials by:

$$a^3 = \frac{3}{4} \frac{PR}{E^*} \quad (1.2a)$$

The quantity  $E^*$  combines the modulus of the indenter and the specimen and is given by<sup>3</sup>:

$$\frac{1}{E^*} = \frac{(1-\nu^2)}{E} + \frac{(1-\nu'^2)}{E'} \quad (1.2b)$$

where the primed terms apply to the indenter properties.  $E^*$  is often referred to as the “reduced modulus” or “combined modulus” of the system. If both contacting bodies have a curvature, then  $R$  in the above equations is their relative radii given by:

$$\frac{1}{R} = \frac{1}{R_1} + \frac{1}{R_2} \quad (1.2c)$$

In Eq. 1.2c the radius of the indenter is set to be positive always, and the radius of the specimen to be positive if its center of curvature is on the opposite side of the lines of contact between the two bodies.

It is important to realize that the deformations at the contact are localized and the Hertz equations are concerned with these and not the bulk deformations and stresses associated with the method of support of the contacting bodies. The deflection  $h$  of the original free surface in the vicinity of the indenter is given by:

$$h = \frac{1}{E^*} \frac{3}{2} \frac{P}{4a} \left( 2 - \frac{r^2}{a^2} \right) \quad r \leq a \quad (1.2d)$$

It can be easily shown from Eq. 1.2d that the depth of the circle of contact beneath the specimen free surface is half of the total elastic displacement. That is, the distance from the specimen free surface to the depth of the radius of the circle of contact at full load is  $h_a = h_p = h_t/2$ :

The distance of mutual approach of distant points in the indenter and specimen is calculated from

$$\delta^3 = \left( \frac{3}{4E^*} \right)^2 \frac{P^2}{R} \quad (1.2e)$$

Substituting Eq. 1.2d into 1.2a, the distance of mutual approach is expressed as:

$$\delta = \frac{a^2}{R} \quad (1.2f)$$

For the case of a non-rigid indenter, if the specimen is assigned a modulus of  $E^*$ , then the contact can be viewed as taking place between a rigid indenter of radius  $R$ .  $\delta$  in Eq. 1.2e becomes the total depth of penetration  $h_t$  beneath the specimen free surface. Rearranging Eq. 1.2e slightly, we obtain:

$$P = \frac{4}{3} E^* R^{1/2} h_t^{3/2} \quad (1.2g)$$

Although the substitution of  $E^*$  for the specimen modulus and the associated assumption of a rigid indenter of radius  $R$  might satisfy the contact mechanics of the situation by Eqs. 1.2a to 1.2g, it should be realized that for the case of a non-rigid indenter, the actual deformation experienced by the specimen is that obtained with a contact with a rigid indenter of a larger radius  $R^+$  as shown in Fig. 1.2. This larger radius may be computed using Eq. 1.2a with  $E'$  in Eq. 1.2b set as for a rigid indenter. In terms of the radius of the contact circle  $a$ , the equivalent rigid indenter radius is given by<sup>4</sup>:

$$R^+ = \frac{4a^3 E}{3(1 - \nu^2) P} \quad (1.2h)$$

There have been some concerns raised in the literature<sup>5</sup> about the validity of the use of the combined modulus in these equations but these have been shown to be invalid.<sup>4,6</sup> Even if the deformation of the indenter is accounted for, the result, correctly interpreted, is equivalent to a rigid indenter in contact with a compliant specimen.

The mean contact pressure,  $p_m$ , is given by the indenter load divided by the contact area and is a useful normalizing parameter, which has the additional virtue of having actual physical significance.

$$p_m = \frac{P}{\pi a^2} \quad (1.2i)$$

Combining Eqs. 1.2a and Eq. 1.2i, we obtain:

$$p_m = \left( \frac{4E^*}{3\pi} \right) \frac{a}{R} \quad (1.2j)$$

The mean contact pressure is often referred to as the “indentation stress” and the quantity  $a/R$  as the “indentation strain.” This functional relationship between  $p_m$  and  $a/R$  foreshadows the existence of a stress–strain response similar in nature to that more commonly obtained from conventional uniaxial tension and compression tests. In both cases, a fully elastic condition yields a linear response. However, owing to the localized nature of the stress field, an *indentation* stress–strain relationship yields valuable information about the elastic–plastic properties of the test material that is not generally available from uniaxial tension and compression tests.

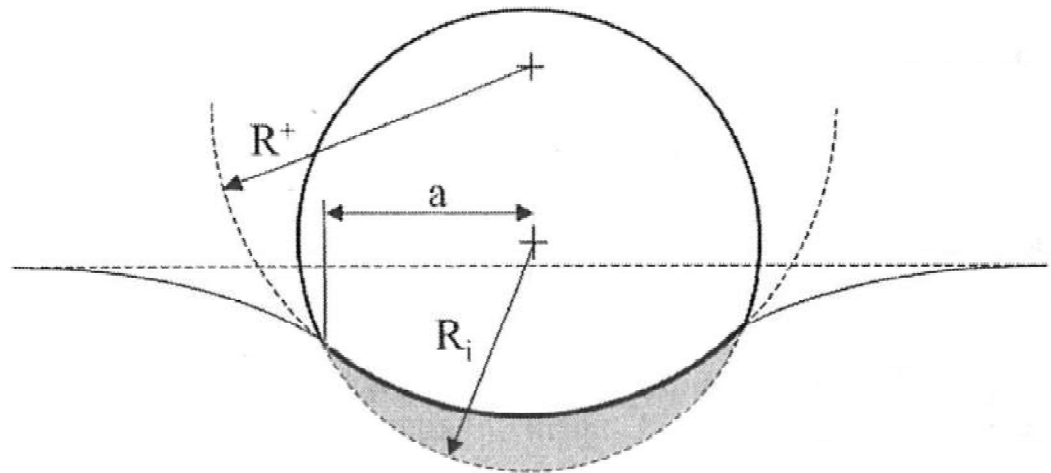


**Fig. 1.2** Contact between a non-rigid indenter and the flat surface of a specimen with modulus  $E$  is equivalent to that, in terms of distance of mutual approach, radius of circle of contact, and indenter load, as occurring between a rigid indenter of radius  $R_i$  and a specimen with modulus  $E^*$  in accordance with Eq. 1.2a. However, physically, the shaded volume of material is not displaced by the indenter and so the contact could also be viewed as occurring between a rigid indenter of radius  $R^+$  and a specimen of modulus  $E$  (Courtesy CSIRO).

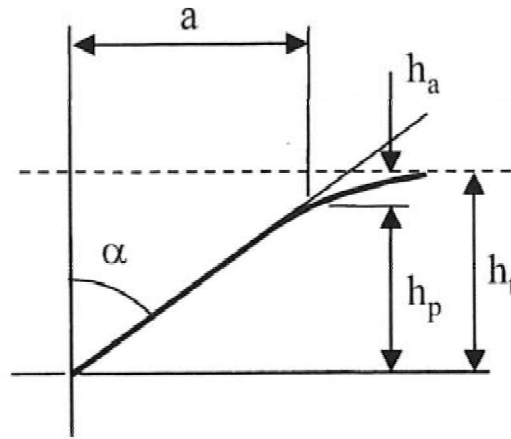


**Fig. 1.3** Geometry of contact with conical indenter.

For a conical indenter, similar equations apply where the radius of circle of contact is related to the indenter load by<sup>7</sup>:

$$P = \frac{\pi a}{2} E^* a \cot \alpha \quad (1.2k)$$

The depth profile of the deformed surface within the area of contact is:

$$h = \left( \frac{\pi}{2} - \frac{r}{a} \right) a \cot \alpha \quad r \leq a \quad (1.2l)$$

where  $\alpha$  is the cone semi-angle as shown in Fig. 1.3. The quantity  $a \cot \alpha$  is the depth of penetration  $h_p$  measured at the circle of contact. Substituting Eq. 1.2k into 1.2l with  $r = 0$ , we obtain:

$$P = \frac{2E^* \tan \alpha}{\pi} h_t^2 \quad (1.2m)$$

where  $h_t$  is the depth of penetration of the apex of the indenter beneath the original specimen free surface.

In indentation testing, the most common types of indenters are spherical indenters, where the Hertz equations apply directly, or pyramidal indenters. The most common types of pyramidal indenters are the four-sided Vickers indenter and the three-sided Berkovich indenter. Of particular interest in indentation testing is the area of the contact found from the dimensions of the contact perimeter. For a spherical indenter, the radius of the circle of contact is given by:

$$\begin{aligned} a &= \sqrt{2R_i h_p - h_p^2} \\ &\approx \sqrt{2R_i h_p} \end{aligned} \quad (1.2n)$$

where  $h_p$  is the depth of the circle of contact as shown in Fig. 1.1. The approximation of Eq. 1.2n is precisely that which underlies the Hertz equations (Eqs. 1.2a and 1.2d) and thus these equations apply to cases where the deformation is small, that is, when the depth  $h_p$  is small in comparison to the radius  $R_i$ .

For a conical indenter, the radius of the circle of contact is simply:

$$a = h_p \tan \alpha \quad (1.2o)$$

**Table 1.1** Projected areas, intercept corrections, and geometry correction factors for various types of indenters. The semi-angles given for pyramidal indenters are the face angles with the central axis of the indenter.

Indenter type	Projected area	Semi-angle $\theta$ (deg)	Effective cone angle $\alpha$ (deg)	Intercept factor* $\epsilon$	Geometry correction factor $\beta$
Sphere	$A \approx \pi 2R h_p$	N/A	N/A	0.75	1
Berkovich	$A = 3\sqrt{3}h_p^2 \tan^2 \theta$	$65.27^\circ$	$70.3^\circ$	0.75	1.034
Vickers	$A = 4h_p^2 \tan^2 \theta$	$68^\circ$	$70.3^\circ$	0.75	1.012
Knoop	$A = 2h_p^2 \tan \theta_1 \tan \theta_2$	$\theta_1 = 86.25^\circ$ , $\theta_2 = 65^\circ$	$77.64^\circ$	0.75	1.012
Cube Corner	$A = 3\sqrt{3}h_p^2 \tan^2 \theta$	$35.26^\circ$	$42.28^\circ$	0.75	1.034
Cone	$A = \pi h_p^2 \tan^2 \alpha$	$\alpha$	$\alpha$	0.727	1

In indentation testing, pyramidal indenters are generally treated as conical indenters with a cone angle that provides the same area to depth relationship as the actual indenter in question. This allows the use of convenient axial-symmetric elastic equations, Eqs. 1.2k to 1.2m, to be applied to contacts involving non-axial-symmetric indenters. Despite the availability of contact solutions for pyramidal punch problems,<sup>8,9,10</sup> the conversion to an equivalent axial-symmetric has found a wide acceptance.

The areas of contact as a function of the depth of the circle of contact for some common indenter geometries are given in Table 1.1 along with other information to be used in the analysis methods shown in Chapter 3.

\* The intercept factors given here are those most commonly used. The values for the pyramidal indenters should theoretically be 0.72 but it has been shown that a value of 0.75 better represents experimental data (see Chapter 3).